HIPERLAN-like Turbo Coded Multi-user Detection Assisted OFDM Based Interactive Video Telephony

P. Cherriman, M. Münster, L. Hanzo
Dept. of ECS, Univ. of Southampton, SO17 1BJ, UK.
Tel: +44-2380-593 125, Fax: +44-2380-593 045
Email: lh@ecs.soton.ac.uk; http://www-mobile.ecs.soton.ac.uk

Abstract—**Multiuser detection assisted, multiple transmit antenna based OFDM arrangements are studied in the context of HIPERLAN 2-like systems. It is demonstrated that the system's user capacity can be improved with the aid of unique spatial user signatures, hence supporting a multiplicity of users. The Maximum Likelihood Sequence Estimation (MLSE) detection algorithm outperformed the Minimum Mean Square Error (MMSE) scheme by about 5dB in terms of the required Signal-to-Noise Ration (SNR) and this performance gain manifested itself also in terms of the system's improved video performance.**

I. BACKGROUND

Recently intensive research efforts have been dedicated to combining Orthogonal Frequency Division Multiplexing (OFDM) [1] with multiple-antenna reception assisted co-channel interference suppression. Since unique user-specific transmit antennas associated with unique user-specific spatial signatures are used, these arrangements are also referred to as Space-Division Multiple Access (SDMA) schemes. One of the key issues is the separation of different users, which can be performed based on their spatial signature, based on the knowledge of the channel parameters. A multiplicity of algorithms has been proposed for performing the task of user separation. The so-called Sample-Matrix Inversion (SMI) [2, 3] algorithm's roots date back to the early years of development in this research area. Other related algorithms, which have recently drawn interest are for example the Successive Interference Cancellation (SIC) technique originally proposed in the context of Lucent's V-BLAST system advocated by Foschini *et al.* in [4, 5]. These techniques were further considered by Vandenameele *et al.* [6] and by Münster *et al.* [7], respectively. Furthermore, a Parallel Interference Cancellation (PIC) algorithm has been considered in [7], while Maximum-Likelihood (ML) combining and potential complexity reduction strategies were discussed by Awater *et al.* in [13]. A similar contribution was presented by Speth *et al.* in [14], where in contrast to [13], the focus is on the problem of maximum likelihood soft-bit generation. A comparative study of these detection schemes was also presented in [7], which concluded that MMSE combining has the lowest-complexity and hence it is the least effective detection scheme. The best performance was exhibited by the ML combiner at the cost of a substantially increased complexity, particularly in the context of higher-order modulation schemes, such as 16QAM. The complexity of PIC and SIC was observed to be within these two boundaries, with an advantage in favour of SIC, specifically in high-complexity scenarios, such as for example in conjunction with four receiver antennas, potentially supporting four simultaneous users. Hence, we opted for focussing our further investigations on the MMSE antenna-array output combining- and the ML combining schemes, more precisely on the MLSE soft-bit generation approach proposed by Speth *et al.* [14], which was found the be more amenable to our turbo coded transmission scenario.

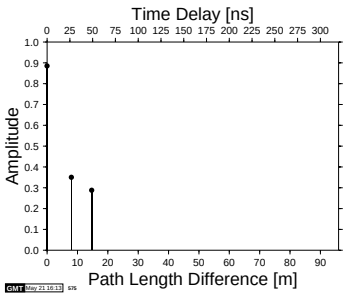

Fig. 1. Short WATM channel impulse response [1].

Due to lack of space here we refrain from detailing the range of developments in the field of wireless video communications and refer the reader to the literature [8]- [12].

This contribution is structured as follows. The description of our OFDM-based video system is given in Section II, which also comprises a discussion of the specific transmission packet structure employed. The MMSE- and ML antenna array output combining strategies are briefly reviewed in Section III, while our modem and video performance results are provided in Section IV for the three-path fading indoor Wireless Asynchronous Transfer Mode (WATM) channel model of Figure 1 [1, 15].

II. THE VIDEO SYSTEM

A. OFDM transceiver

We assume an OFDM-SDMA uplink environment, where the number of co-channel users is upper-bounded by the number of antenna elements associated with the receiver array at the base-station. By contrast, each user is equipped with a single transmission antenna. In our OFDM scheme 512 subcarriers and a 64-sample guard-interval was used, in order to avoid inter-symbol interference. Five consecutive OFDM symbols were hosted by a packet, which was transmitted at specific intervals, in order to fulfill the bitrate requirements of the video codec. The packet structure is portrayed in Figure 2. Specifically, the first OFDM symbol of a packet is a dedicated training symbol, hosting exclusively pilot tones, while the following four OFDM symbols host exclusively data symbols. More specifically, the training OFDM symbol exhibits the structure illustrated in Fig-

0-7803-7005-8/01/$10.00 (c) 2001 IEEE

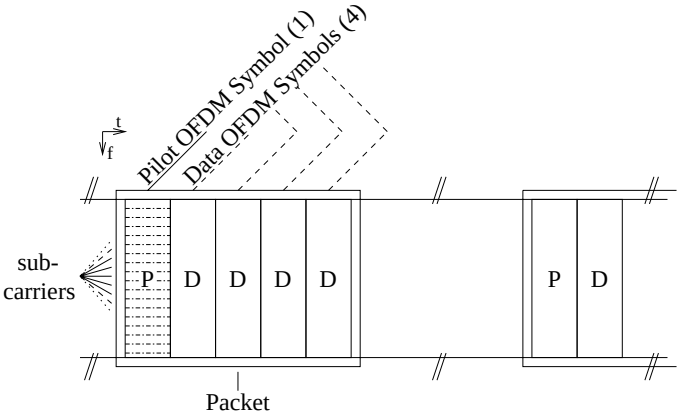

Fig. 2. Packet structure of the proposed multi-user video transmission arrangement. A dedicated pilot OFDM symbol is transmitted at the beginning of the five-symbol burst, followed by a set of four OFDM symbols hosting exclusively data subcarriers.

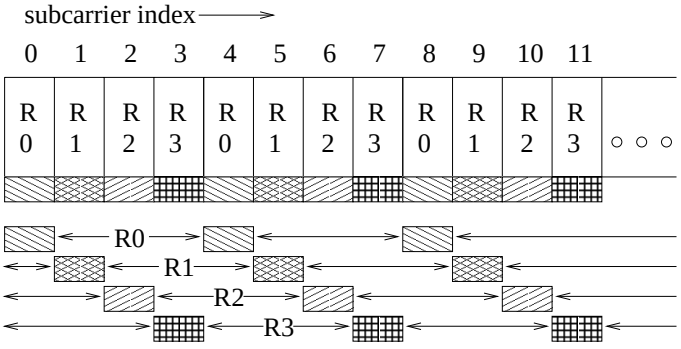

Fig. 3. Pilot arrangement hosted by the first OFDM symbol in the video packet for simultaneously estimating the channel transfer functions between the different users' transmit antennas and the multiple array elements at the Base Station's (BS) receiver.

ure 3, potentially supporting four simultaneous users.

There are two typical types of pilot arrangements, as seen at the top and bottom of Figure 3, respectively. These can be differentiated on the basis, whether the different users are assigned separate dedicated pilot positions, or whether the pilots are spread over several subcarriers. Specifically, in case of separate dedicated pilot positions, as portrayed at the top of Figure 3, the l-th of the four users supported would transmit pilot tones at the subcarrier positions indicated by R_{l-1} $l = 1 \ldots 4$ in Figure 3, while transmitting no pilot symbols at the other subcarrier frequencies. At the receiver MMSE lowpass interpolation is performed separately for generating a channel transfer function estimate for equalising the frequency-domain signals received by the different antenna array elements associated with the different users. Again, this is carried out separately between all pilot symbols of the same relative index $l-1$ associated with the l-th user, as seen at the top of Figure 3. This low-pass interpolation procedure allows us to generate a subcarrier by subcarrier based estimate of the channel's frequency-domain transfer function between the single transmit antenna of the l-th user and the reception antenna array element considered.

The second pilot arrangement seen at the bottom of Figure 3 allows the different users' pilots to share a number of pilot positions. This is achieved upon invoking the principles of orthogonal code-division. Specifically, spreading can be implemented by means of assigning an individual orthogonal code to each user. The l-th user would hence spread each single pilot tone across several subcarriers, namely four subcarriers in Figure 3, in all consecutive four subcarrier block hosting indices R_0-R_3. At the receiver, again, interpolation is carried out separately across the subcarriers having the same relative index R_i, followed by cross-correlation with the user's individual spreading codes, in order to extract the different users' channel transfer functions.

Both of the above pilot-based channel estimation methods of Figure 3 are capable of achieving the same estimation performance, provided that in the case of dedicated non-spread pilot tones each user is allowed to boost its transmit power by a factor equal to the number of simultaneous users. This power-boosting measure can be invoked, since - as outlined before - no symbols are transmitted on subcarriers between the pilot positions. The expected difference between the above-mentioned two methods is their different Peak-to-Average Power Ratio (PAPR) at the output of the OFDM modulator - an issue, which requires further investigations.

Throughout the simulations conducted in Section IV we assumed 'packet-invariant' fading, where again, a packet was constituted by five OFDM symbols. Accordingly, the fading magnitude and phase was considered constant during the packet hosting a total of five OFDM symbols. This assumption is justified by the low OFDM symbol-normalized Doppler frequency of $F_d = 1.532 \cdot 10^{-3}$ encountered in the indoor WATM channel scenario of [1] at the maximum pedestrian speed of $3m/s$, which was assumed here.

Furthermore, for our simulations we assumed that the fading experienced by consecutive video packets was uncorrelated, which is justified by the relatively high time-domain separation between two consecutive video packets at the bitrates envisaged. In addition, a turbo convolutional codec has been incorporated into the system, which resulted in a substantial Bit Error Ratio (BER) reduction. The turbo coding parameters can be summarized as follows. The coding rate was $R = 1/2$, the constraint length was $K = 3$, the octally represented generator-polynomials of $\{7, 5\}$ were used, and four turbo decoding iterations were performed.

B. Video Transmission Regime

In this contribution we transmitted 176x144 pixel Quarter Common Intermediate Format (QCIF) video sequences at 30 frames/s using the above OFDM transceiver, which can be configured as a 1, 2 or 4 bit/symbol scheme. The H.263 video codec was used [8], which extensively employs variable-length compression techniques and hence achieves a high compression ratio. However, as all entropy- and variable-length coded bit streams, its bits are extremely sensitive to transmission errors.

This error sensitivity was counteracted in our system by invoking an adaptive packetisation and packet dropping regime, when the channel codec protecting the video stream became incapable of removing all channel errors. Specifically, we refrained from decoding the corrupted video packets in order to

Features	Multi-rate system		
Mode	BPSK	4QAM	16QAM
Coded data bits/packet	254	510	1020
Packet Rate (packets/s)	976.560000		
Transmission data bitrate (kbit/s)	248.0	498.0	996.1
Video packet CRC (bits)	16		
Feedback protection (bits)	15		
Video packet header (bits)	9	10	11
Video bits/packet	214	469	978
Effective Video-rate (kbit/s)	209.0	458.0	955.1
Video framerate (Hz)	30		

TABLE I
VIDEO SYSTEM PARAMETERS

prevent error propagation through the reconstructed video frame buffer [8, 9]. Hence these corrupted video packets were dropped at both the transmitter and receiver and the reconstructed frame buffer was not updated, until the next error-free video packet replenishing the specific video frame area was received. This required a low-delay, strongly protected video packet acknowledgement flag, which was superimposed on the transmitted payload packets [8, 9]. The associated video performance degradation was found perceptually unobjectionable for Packet Loss Rates (PLR) below about 5%, although this issue will be detailed in more depth during our further discourse. Due to lack of space some of the implementational details of the video packetisation and transmission regime are omitted, which can be found in [8, 9].

More xeplicitly, the H.263 decoder discards all the corrupted video packets. A 16 bit Cyclic Redundancy Check (CRC) is added to every video packet for detecting corrupted packets. In addition to the CRC, each video packet has a header, containing information which allows the packet disassembly block to appropriately combine the macroblocks' video information, which has been mapped to and transmitted in several consecutive video transmission packets. The video encoder receives feedback information from the decoder, informing it of the success or failure of the previous packet. In case of corruption the packet disassembly block effectively conceals the packet loss by replacing the affected area of the picture with the corresponding area from the previous video frame.

In addition to rendering the video information more robust against channel errors, the packet assembly and disassembly block is capable of assembling video packets containing more bits, when higher order modulation modes are used in case of a high instantaneous channel quality. The bitrate control mechanism of the video encoder is closely linked to the packet assembly block, in order to compensate for the rapid changes in the QAM transmission mode and the resultant packet size. The video system's parameters are summarised in Table I.

III. CO-CHANNEL INTERFERENCE CANCELLATION TECHNIQUES

In this section we provide a brief overview of the two antenna array output combining strategies considered here, specifically

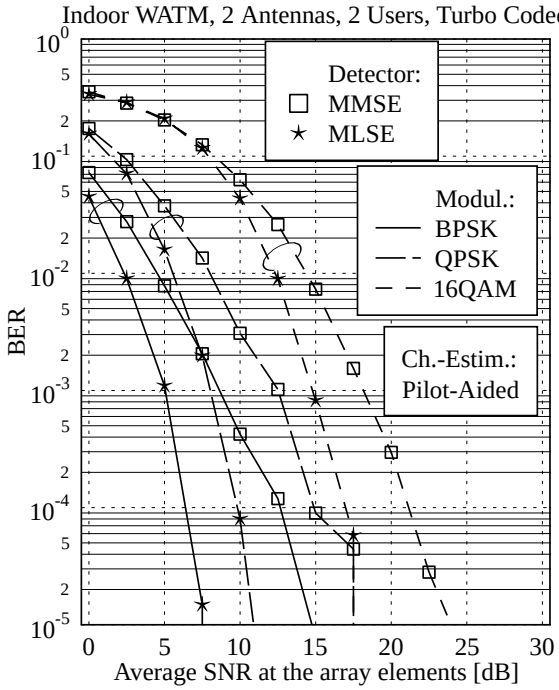

Fig. 4. BER versus channel SNR performance of the turbo coded OFDM system using MMSE or ML array output combining at the **two-element** antenna array assisted receiver. Two simultaneous users of equal signal power were supported in the 1, 2 and 4 bit/symbol modulation modes when using pilot-aided channel estimation according to Figures 2 and 3 over the WATM channel of Figure 1

that of MMSE combining and ML combining.

The SMI-Algorithm - The SMI algorithm [2, 3] generates the optimum antenna array weights in the sense of the Minimum Mean Square Error (MMSE) between the associated combiner's output signal and a reference signal known to the receiver.

The MLSE-Algorithm - The second algorithm studied is the MLSE soft-bit generation algorithm proposed by Speth *et al.* in [14]. This technique constitutes a derivative of the ML combiner, which can be employed in both channel coded- and uncoded systems after applying hard-decisions to the so-called Log-Likelihood Ratios (LLR) of the bits. This approach is based on the idea of detecting one out of L users at a time, so as to avoid the complex joint detection of all users by a Viterbi-like tree-search based detector.

IV. VIDEO SYSTEM PERFORMANCE RESULTS

Again, the video system's parameters are summarised in Table I. The two-antenna, two-user system's BER versus channel SNR performance is shown in Figure 4, indicating that the MLSE algorithm consistently outperforms the MMSE algorithm. When the number of users and antennas is increased to four, the BER performance results of Figure 5 are obtained for the more powerful MMSE combiner. Observe that the four-

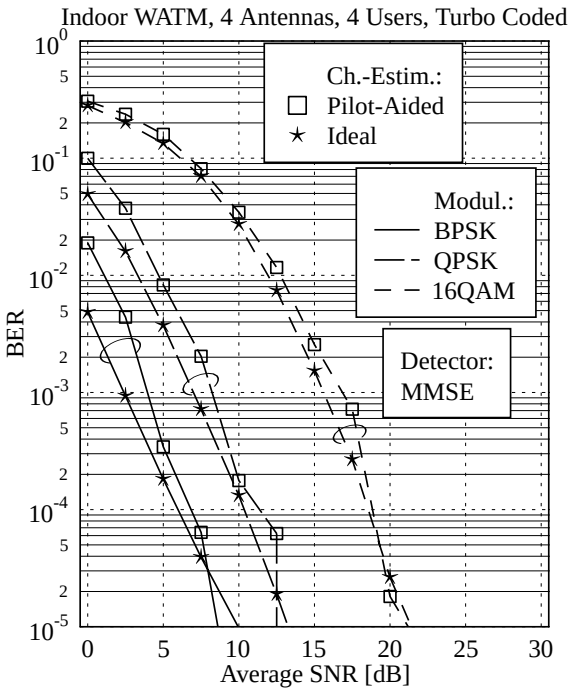

Fig. 5. BER versus channel SNR performance of the turbo coded OFDM system using MMSE or ML array output combining at the **four-element** antenna array assisted receiver. Four simultaneous users of equal signal power were supported in the 1, 2 and 4 bit/symbol modulation modes when using pilot-aided channel estimation according to Figures 2 and 3 over the WATM channel of Figure 1

antenna scenario performs better, since the four transmit and four receiv antennas create a total of 16 virtual channels instead of the four virtual channels associated with the two transmitter and two receiver scenario. Hence in the former system a higher grade of diversity can be provided by the system.

In our further discourse the effective video throughput bitrate is defined as the video bitrate provided by the correctly received packets, since the erroneously received packets are discarded. Therefore, the effective thoughput bitrate is that of the decoded error-free video stream, which is shown in Figure 6 as a function of the channel SNR.

The average Peak-Signal-to-Noise-Ratio (PSNR) objective video quality metric was invoked in Figure 7 in order to demonstrate that the average video quality degrades, as the PLR increases. Our informal subjective video quality investigations indicated that video PSNR degradations of 1-2dB are unobjectionable, suggesting that the system is capable of operating at PLRs of up to about 5%. When the PLR monitored by the system exceeds the above threshold value, the transceiver is instructed by the system controller to switch to a more robust modulation mode, say from 4 bit/symbol to 2 and 1 bit/symbol, before the subjective video quality becomes noticably degraded.

In order to provide a further perspective on the MMSE and MLSE assisted system's performance, Figure 8 characterises

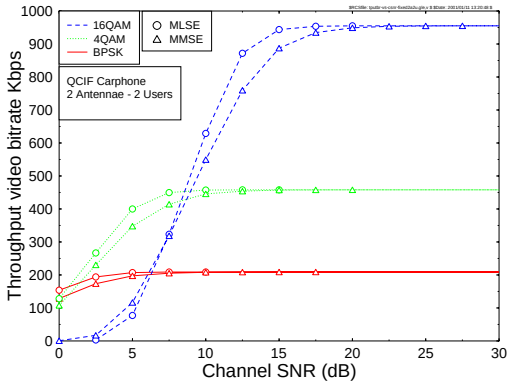

Fig. 6. Effective video throughput bitrate versus channel SNR for the **two-antenna, two-user** OFDM system for transmission over the WATM channel of Figure 1.

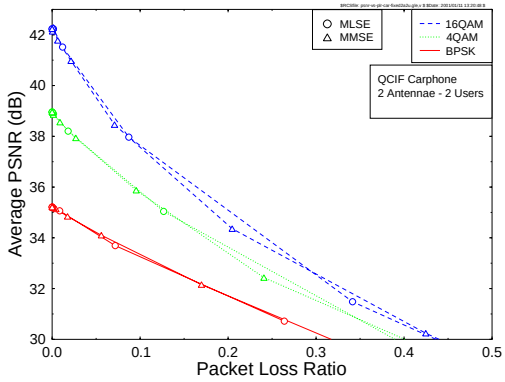

Fig. 7. Average PSNR versus PLR of the **two-antenna, two-user** OFDM scheme for transmission over the WATM channel of Figure 1.

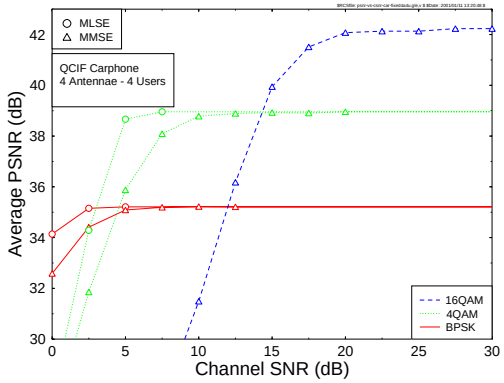

Fig. 8. Average PSNR versus channel SNR performance of the **four-antenna, four-user** OFDM system for transmission over the WATM channel of Figure 1.

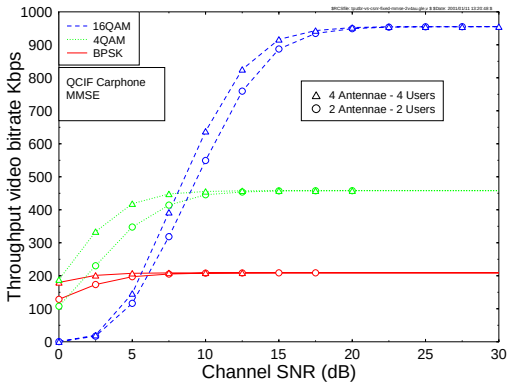

Fig. 9. Effective video throughput bitrate versus channel SNR using the MMSE OFDM scheme for a **two-antenna, two-user scenario and for a four-antenna, four-user** scenario for transmission over the WATM channel of Figure 1.

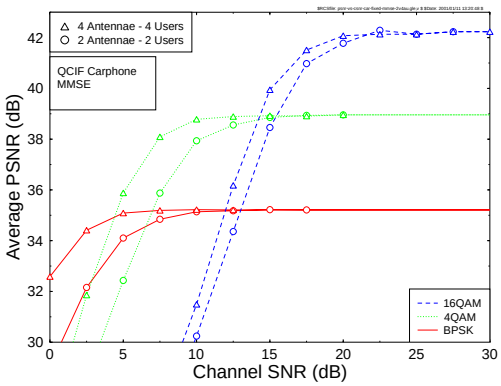

Fig. 10. Average PSNR versus channel SNR performance of the MMSE OFDM scheme for **two-antenna, two-user and for four-antenna, four-user** scenarios for transmission over the WATM channel of Figure 1.

the achievable video performance in terms of the PSNR. Figure 9 shows the effective video throughput bitrate versus channel SNR performance for the MMSE system, supporting two- and four-users. Again, the four-antenna, four-user system exhibits a better performance. However, as before, the throughput bitrate difference between the two- and four-user systems is modest, except when the bitrate starts to degrade, as the channel SNR degrades.

Although due to lack of space the corresponding results are not shown here, we found that the performance difference between the two- and four-antenna scenarios was higher for the lower-order modulation modes and the performance difference decreased, as the number of bits per modulated symbol is increased. The corresponding average PSNR or video quality versus channel SNR graph is shown in Figure 10, quantifying the video performance difference of the two- and four-antenna scenarios. Again, the performance difference reduces, as the modulation order is increased.

V. Summary and Conclusions

Multiuser detection assisted, multiple transmit antenna based OFDM schemes were studied in the context of HIPERLAN 2-like systems. It was demonstrated that the system's user capacity can be improved with the aid of unique spatial user signatures. Hence a multiplicity of users can be supported. The MLSE detection algorithm outperformed the MMSE scheme by about 5dB in terms of the required SNR and this performance gain manifested itself also in terms of the system's video performance.

References

[1] L. Hanzo, W. Webb, and T. Keller, *Single- and Multi-carrier Quadrature Amplitude Modulation*. IEEE Press-Pentech Press, April 2000.

[2] Y. Li and N. R. Sollenberger, "Adaptive Antenna Arrays for OFDM Systems with Cochannel Interference," *IEEE Trans. on. Comms.*, vol. 47, pp. 217–229, Feb 1999.

[3] M. Münster, T. Keller, and L. Hanzo, "Co–Channel Interference Suppression Assisted Adaptive OFDM in Interference Limited Environments," in *Proc. of Vehicular Technology Conference*, vol. 1, (Amsterdam, Netherlands), pp. 284–288, IEEE, September 19-22 1999.

[4] G. J. Foschini, "Layered Space-Time Architecture for Wireless Communication in a Fading Environment when using Multi-Element Antennas"," *Bell Labs Technical Journal*, vol. Autumn, pp. 41–59, 1996.

[5] G. D. Golden, G. J. Foschini, R. A. Valenzuela, and P. W. Wolniansky, ""Detection Algorithms and Initial Laboratory Results using V-BLAST Space-Time Communication Architecture"," *IEE Electronics Letters*, vol. 35, pp. 14–16, Jan. 1999.

[6] P. Vandenameele, L. V. der Perre, M. Engels, and H. D. Man, "A Novel Class of Uplink OFDM/SDMA Algorithms for WLAN," in *Proc. of Global Telecommunications Conference - Globecom'99*, vol. 1, (Rio de Janeiro, Brazil), pp. 6–10, IEEE, December 5-9 1999.

[7] M. Münster and L. Hanzo, "Co-Channel Interference Cancellation Techniques for Antenna Array Assisted Multiuser OFDM Systems," in *Proceedings of 3G-'2000 Conference*, vol. 1, (London, Great Britain), pp. 256–260, IEE, IEE, March 27-29 2000.

[8] L. Hanzo, P. Cherriman, and J. Streit, "Wireless video communications: Second to third generation beyond." IEEE Press, 2001 (For detailed contents please refer to http://www-mobile.ecs.soton.ac.uk.).

[9] P. Cherriman and L. Hanzo, "Programmable H.263-based wireless video transceivers for interference-limited environments," *IEEE Transactions on Circuits and Systems for Video Technology*, vol. 8, pp. 275–286, June 1998.

[10] L. Hanzo, C. Wong, and P. Cherriman, "Channel-adaptive wideband video telephony," *IEEE Signal Processing Magazine*, vol. 17, pp. 10–30, July 2000.

[11] L. Hanzo, P. Cherriman, and E. Kuan, "Interactive cellular and cordless video telephony: State-of-the-art, system design principles and expected performance," *Proceedings of IEEE*, September 2000, pp 1388-1413

[12] P. Cherriman, C.H. Wong, L. Hanzo: Turbo- and BCH-coded Wideband Burst-by-burst Adaptive H.263-Assisted Wireless Video Telephony; IEEE Tr. on CSVT, 2000, Vol. 10, No 10, Dec. 2000, pp 1355-1363

[13] G. Awater, A. v. Zelst, and R. v. Nee, "Reduced Complexity Space Division Multiplexing Receivers," in *Proc. of Vehicular Technology Conference*, vol. 1, (Tokyo, Japan), pp. 11–15, IEEE, May 15-18 2000.

[14] M. Speth, A. Senst, and H. Meyr, "Low Complexity Space-Frequency MLSE for Multi-User COFDM," in *Proc. of Global Telecommunications Conference - Globecom'99*, vol. 1, (Rio de Janeiro, Brazil), pp. 2395–2399, IEEE, December 5-9 1999.

[15] T. Keller and L. Hanzo, "Adaptive Orthogonal Frequency Division Multiplexing Schemes," in *Proceedings of ACTS'98 Summit*, (Rhodos, Greece), pp. 794–799, June 1998.